









RESEARCH ARTICLE

10.1029/2022GC010647

Trace Element Geochemistry in the Earliest Terrestrial Ecosystem, the Rhynie Chert

John Parnell¹ , Temitope O. Akinsanpe^{1,2} , Joseph G. T. Armstrong¹ , Adrian J. Boyce³, John W. Still¹, Stephen A. Bowden¹, David Clases⁴ , Raquel Gonzalez de Vega⁴ , and Joerg Feldmann⁴ 

¹School of Geosciences, University of Aberdeen, Aberdeen, UK, ²Obafemi Awolowo University, Ile Ife, Nigeria, ³Scottish Universities Environmental Research Centre, Glasgow, UK, ⁴TESLA, Institute of Chemistry, University of Graz, Graz, Austria

Key Points:

- The plant-bearing Rhynie Chert contains authigenic mineral phases, including pyrite, and manganese-iron and titanium oxides
- Authigenic phases may be products of bacterial and fungal components and sequestered potentially toxic elements, including As, Sb, and W
- Detrital monazite was leached to supply phosphate, which was required by fungi in symbiosis with plants

Correspondence to:

J. Parnell,
J.Parnell@abdn.ac.uk

Citation:

Parnell, J., Akinsanpe, T. O., Armstrong, J. G. T., Boyce, A. J., Still, J. W., Bowden, S. A., et al. (2022). Trace element geochemistry in the earliest terrestrial ecosystem, the Rhynie Chert. *Geochemistry, Geophysics, Geosystems*, 23, e2022GC010647. <https://doi.org/10.1029/2022GC010647>

Received 3 AUG 2022
Accepted 7 DEC 2022

Author Contributions:

Conceptualization: John Parnell
Data curation: Temitope O. Akinsanpe
Formal analysis: Temitope O. Akinsanpe, Joseph G. T. Armstrong, John W. Still, David Clases, Raquel Gonzalez de Vega
Investigation: John Parnell
Methodology: John Parnell, Temitope O. Akinsanpe
Supervision: John Parnell
Validation: Adrian J. Boyce, Stephen A. Bowden, Joerg Feldmann
Writing – original draft: John Parnell
Writing – review & editing: John Parnell

© 2022. The Authors.

This is an open access article under the terms of the [Creative Commons Attribution License](https://creativecommons.org/licenses/by/4.0/), which permits use, distribution and reproduction in any medium, provided the original work is properly cited.

Abstract The symbiotic partnership of plants and fungi was a critical means of nutrient uptake during colonization of the terrestrial surface. The Lower Devonian Rhynie Chert shows evidence for extensive phosphorus mobilization in plant debris that was pervasively colonized by fungi. Sandy sediment entrapped with fungi-rich phytodebris contains grains of the phosphate mineral monazite which exhibit alteration to highly porous and leached surfaces. Mixed manganese-iron oxide precipitates contain up to 2% P₂O₅. The mobilization of Mn, Fe, and P are all features of mycorrhizal nutrient concentration. However, the ecosystem was also exposed to toxic elements from hot spring hydrothermal activity. The oxide precipitates include titanium and iron-titanium oxide which sequestered potentially toxic tungsten and antimony. Abundant pyrite framboids in the Rhynie Chert indicate that plant decomposition included microbial sulfate reduction. This caused the removal of some of the arsenic from the groundwaters into the pyrite, which reduced toxicity while leaving enough for putative arsenic metabolism. These relationships show the mineral component of the ecosystem modified the geochemistry of ambient waters.

Plain Language Summary The symbiotic partnership of plants and fungi was a critical means of nutrient uptake during colonization of the terrestrial surface. The Lower Devonian Rhynie Chert shows evidence for extensive phosphorus mobilization in plant debris that was pervasively colonized by fungi. Sandy sediment entrapped with fungi-rich organic matter contains grains of the phosphate mineral monazite which exhibit alteration to highly porous and leached surfaces. The ecosystem was also exposed to toxic elements from hot springs. Precipitates of oxide minerals sequestered potentially toxic tungsten and antimony. Iron sulfide allowed the removal of excess arsenic from the groundwaters. These relationships show the mineral component of the ecosystem modified the geochemistry of ambient waters.

1. Introduction

The Rhynie Chert (Figure 1) is a Lower Devonian (~407 Ma) lagerstätte of early plants and their accompanying biota (Strullu-Derrien et al., 2014; Trewin & Fayers, 2015), preserved by early silicification from adjacent hot spring activity (Baron et al., 2004). The deposit constitutes the world's oldest preserved terrestrial ecosystem, including extensive evidence for the colonization of plants by mycorrhizal fungi (Harper et al., 2020; Krings et al., 2018; Strullu-Derrien et al., 2014; Taylor et al., 2004). Arbuscular mycorrhizal fungi evolved in symbiosis with early plants which were colonizing the Devonian land surface (Remy et al., 1994). The plants require trace elements, supplied by the fungi, while the fungi gain carbon from the photosynthesizing plant. Fungi similarly controlled nutrients that were required by animals in the Rhynie ecosystem (Strullu-Derrien et al., 2016). Fungi also contribute to plant resistance against contaminating trace elements (Colpaert et al., 2011; Hildebrandt et al., 2007; Neidhardt, 2020). It is important to note that much current work on the fungal response to metals relates to ectomycorrhizal or ericoid mycorrhizal fungi, which had not evolved at the time of Rhynie Chert deposition. This includes numerous studies on the fungus *Aspergillus*. However, there is also evidence that arbuscular mycorrhizae, which were present at Rhynie, influence the occurrence and speciation of numerous trace elements, including manganese (Garcia et al., 2020), phosphorus (George et al., 1995), titanium (Burghelea et al., 2015), arsenic (Neidhardt, 2020) and antimony (Wei et al., 2016), all of which formed minerals in the Rhynie Chert.

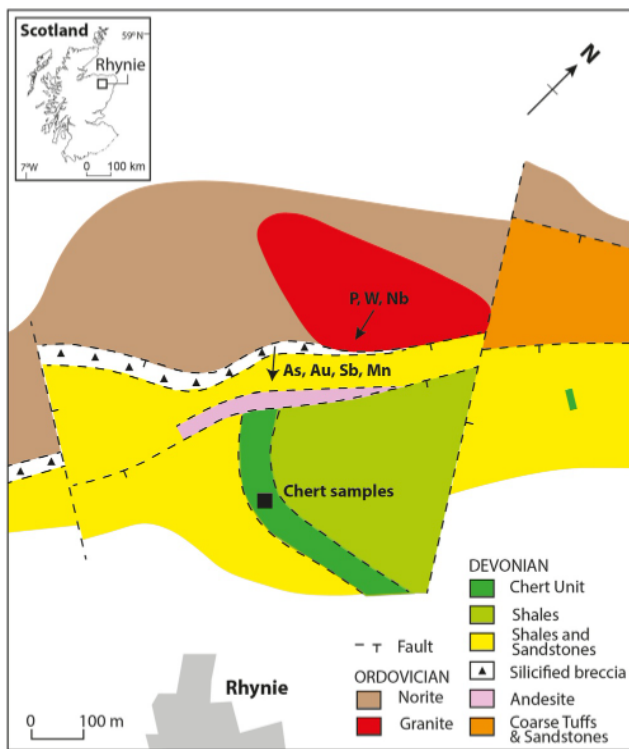


Figure 1. Geological map of region near Rhynie village. Elements contributed to chert from hot spring system represented by silicified breccia, and basement rocks including granite.

The plant-bearing cherts are within a few hundred meters from a silicified, veined, fault zone, the assumed locus of hot spring activity (Figure 2). Limited geochemical data indicate a mixture of hydrothermal and detrital components in the cherts (Rice & Trewin, 1988). Enrichments in arsenic (up to 300 ppm), antimony (up to 71 ppm) and gold (up to 0.25 ppm) are attributable to hydrothermal mineralization of the springs (Rice & Trewin, 1988; Rice et al., 1995). The fault zone is also enriched in manganese, tungsten and molybdenum, and contains moderate vanadium levels (Rice et al., 1995). The arsenic and gold have been attributed to andesitic magmas, and the tungsten to Caledonian plutonic rocks (granite-syenite) adjacent to the fault zone (Parry et al., 2011; Rice et al., 1995), both of which would have been scavenged by the hydrothermal fluids. The tungsten may have a dual source as arsenic, tungsten and antimony are typical components of geothermal water (Stefánsson & Arnórsson, 2005). Two geochemical issues arise from what is known about the Rhynie Chert. First, it is widely hypothesized that the fungi in Rhynie Chert allowed the take-up of phosphorus into the plants (Brundrett et al., 2018; Mills et al., 2018; Taylor et al., 2004), but without supporting evidence for the processing of phosphorus. Second, the anomalous arsenic from the hot springs suggests that early plants had to cope with arsenic toxicity (Channing, 2017; Channing & Edwards, 2009; Meharg, 2002; Meharg & Hartley-Whitaker, 2002), and other elements from the springs such as tungsten are also toxic to plants (Adamakis et al., 2012).

Petrographic studies can show how the balance of elements was achieved. In particular, this study reports:

1. Identification of mineral source(s) of phosphorus.
2. Evidence of mobilization, and thus availability, of phosphorus.
3. Evidence of how the ecosystem responded to high levels of arsenic, antimony and tungsten.

Note we limit our discussion to the incorporation of metals into mineral phases, but additionally fungi have the capacity to bind large amounts of metals to their biomass (Colpaert et al., 2011). It is possible that some mineral-bound trace metals were formerly biomass-bound, before biomass decay.

2. Geological Setting: Host Sediment in Rhynie Chert

The Rhynie Chert occurs with a Lower Devonian continental succession in northern Scotland (Figure 1). The succession consists of sandstones and shales in a kilometer-scale, fault-bounded basin, the Rhynie Basin, within pre-Devonian crystalline basement (Rice et al., 1995; Trewin & Fayers, 2015). The chert forms the Rhynie Cherts Unit, within the Dryden Flags Formation, in the upper part of the succession (Trewin & Fayers, 2015). The basement includes Neoproterozoic metasediments, Ordovician ultramafic intrusions and Caledonian (Silurian-Devonian) plutonic rocks, which all contributed siliciclastic sediment to the basin. The Devonian sediment additionally includes tuffaceous beds and an andesite layer underlying the chert (Figure 1), which represent pencontemporaneous volcanic activity. Associated hot springs engendered silicification of sediment near the Rhynie Fault Zone at the basin margin. The resultant chert contains exceptionally preserved plants, fungi and animals, which have been the subject of extensive study. They represent the oldest preserved terrestrial ecosystem. The Devonian rocks are at upper oil window thermal maturity, that is, vitrinite reflectance up to 1.2% (Wellman, 2006), and are consequently very well preserved.

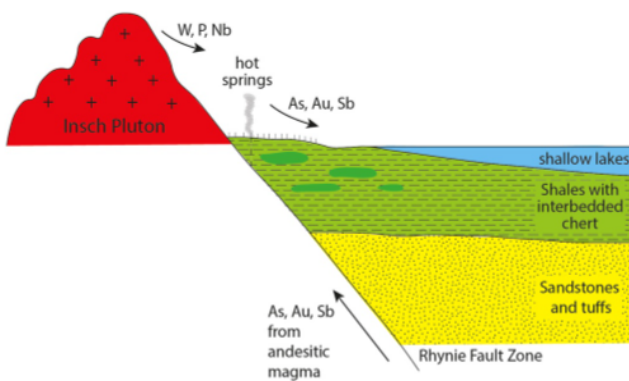


Figure 2. Schematic cross-section showing contribution of elements to Devonian chert-forming environment. Elements sourced from deep-seated magma in Rhynie Fault Zone (As, Sb, Au) and detrital matter eroded from pre-Devonian basement (P, W). Section based on Rice et al. (2002).

The succession is interpreted to represent sedimentation adjacent to a river system where floodplains were periodically inundated, and which included ephemeral lakes (Trewin & Fayers, 2015). The Rhynie Cherts Unit includes over 50 cm-scale chert horizons, with low lateral continuity. The cherts consist of beds of plants in growth position, separated by beds of sediment. All were encased in silica from the springs while plants were still growing (Trewin, 1994; Trewin & Fayers, 2015). The sediment consists of lenses of sand and layers of compressed phytodebris (mainly fragments of plant stems; so-called “litter layers” of Krings et al. [2018]). The phytodebris layers are pervasively colonized by fungi (Krings et al., 2018; Powell et al., 2000). The mineral components consist of detrital grains, and phases precipitated soon after sediment deposition. No red beds are evident in the chert-bearing succession at Rhynie.

The detrital grains consist of fine sand (0.1–0.5 mm), mostly composed of quartz, feldspar, micas and chloritoids, and smaller grains (<50 μm) of heavy minerals including monazite, zircon, staurolite, chromite and garnet. The heavy grains may have percolated down between the sand grains in the manner of fine gold grains trapped within much coarser sand and gravel. The post-depositional mineral phases include mixed manganese and iron oxides, and abundant titanium oxides (rutile) and titanium-iron oxides, in the layers of compacted phytodebris, and pyrite in the plant-bearing beds. Each of the monazite, Mn-Fe oxides, Ti oxides and pyrite had a role to play in the biogeochemistry of the chert.

3. Methods and Materials

Samples were taken from a logged trench section (03/T1), excavated in 2003 (Trewin & Fayers, 2015), supplemented by float material in the trench. Andesite was sampled from borehole 97/8, depth 51.4 m (Rice et al., 2002).

Scanning electron microscopy (SEM) was conducted in the Aberdeen Center for Electron Microscopy, Analysis and Characterization (ACEMAC) facility at the University of Aberdeen using a Carl Zeiss GeminiSEM 300 VP Field Emission instrument equipped with an Oxford Instruments NanoAnalysis Xmax80 Energy Dispersive Spectroscopy (EDS) detector, and AZtec software suite. Standards were supplied by factory, and use elemental Fe, Mn, W, Sb, V, Sc, and Nb, and also GaP for phosphorus and InAs for arsenic. Relevant detection limits are MgO 0.09%, FeO 0.18%, As_2O_3 and P_2O_5 0.3%. Element maps were acquired for 2 hr 45 min.

The degree of pyritization (DOP; dimensionless proportion of iron present as sulfide rather than reactive (acid soluble) iron) was calculated using the technique of Leventhal and Taylor (1990). Specifically, powdered bulk rock was dissolved in 1N HCl for 24 hr to measure the acid soluble fraction. Iron concentration was measured using a Palintest Photometer 7500.

For sulfur isotope analysis, pyrite samples from the Moffat Shale were combusted with excess Cu_2O at 1075°C in order to liberate the SO_2 gas under vacuum conditions. Liberated SO_2 gases were analyzed on a VG Isotech SIRA II mass spectrometer, with standard corrections applied to raw $\delta^{66}\text{SO}_2$ values to produce true $\delta^{34}\text{S}_{\text{CDT}}$ values. The standards employed were the international standard NBS-123, IAEA-S-3, and SUERC standard CP-1.

LA-ICP-MS analyses were performed with an Analyte G2 excimer laser ablation system (Teledyne CETAC Technologies, Omaha, NE, USA) equipped with an aerosol rapid introduction system (ARIS, Teledyne CETAC) and coupled to an Agilent 8900 Triple Quadrupole ICP-MS/MS instrument (Agilent Technologies, Santa Clara, CA, USA). The LA-ICP-MS system was tuned daily for maximum sensitivity analyzing the reference material NIST 612 “Trace Elements in Glass.” The ICP-MS instrument was operated in standard (single quadrupole) mode and tuned to minimize the formation of oxides by monitoring the oxide ratio ($^{232}\text{Th}^{16}\text{O}^+ / ^{232}\text{Th}^+$, m/z 248/232 < 1%). Isotope ratios were monitored to confirm the absence of interfering polyatomic species. The laser beam spot size was adjusted to 30 μm and the frequency to 150 Hz generating a fluence of 3.92 J cm^{-2} at a wavelength of 193 nm. Helium was used as carrier gas with a flow rate of 0.55 L min^{-1} (0.30 L min^{-1} cell gas, 0.25 L min^{-1} ablation cup gas). Image construction was performed using the HDIP software v.1.6.6.d44415e5 (Teledyne).

4. Results

Monazite grains in the sand of the phytodebris layers exhibit a range of compositions (variable proportions of Y, Nd, Gd), which suggests that they are detrital rather than precipitated authigenically. The grain surfaces are very highly modified from the original rounded shapes or crystal faces. The monazite has been altered to apparently recrystallized masses with internal porosity (Figure 3), resulting in orders of magnitude greater surface area than

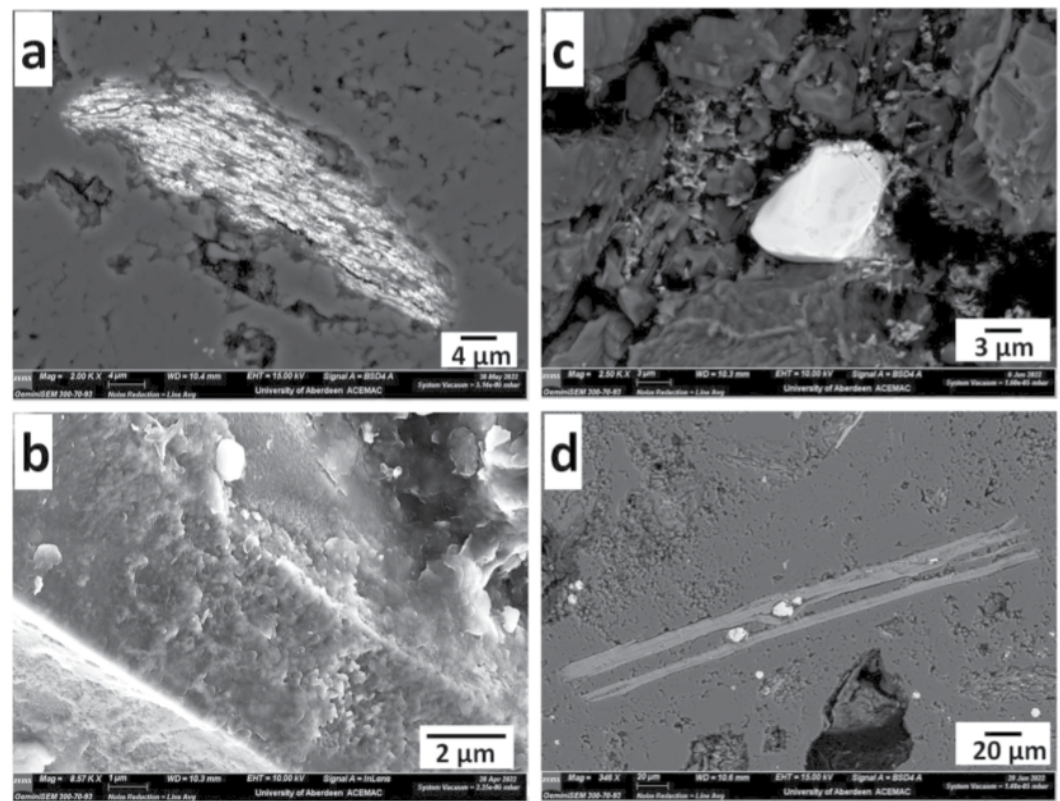


Figure 3. Backscattered scanning electron micrographs of monazite and other minerals in Rhynie Chert. (a) Polished monazite grain, exhibiting unusual degree of alteration; (b) Detail of grain surface showing extensive etching and development of porosity; (c) Monazite in underlying sandstone, relatively unaltered; (d) Biotite in Rhynie Chert, unaltered; shows also titanium oxide crystals (bright).

the original grains. In contrast, other heavy minerals such as zircon exhibit grain surfaces that are rounded and smooth rather than porous. Other less stable minerals in the chert, like biotite, are not altered (Figure 3). Monazite grains in sandstones below the chert-bearing succession are similarly unaltered (Figure 3).

The fungi-bearing phytodebris layers also contain precipitates which cement the organic matter and detrital grains. The cement is a variable mixture of Mn and Fe oxides (Figures 4 and 5), from pure Mn oxide to pure Fe oxide, all containing trace amounts of P, As, and S (Table 1). The P_2O_5 and As_2O_3 contents in the oxide precipitates are up to 2% and 1% respectively. Admixture with clay minerals is represented by variable content of aluminum (Table 1). The titanium oxide (Table 2) occurs in the same layers, as crystals up to 50 μm size with subhedral faces, and contains traces of tungsten (up to 8% WO_3), niobium (up to 2% Nb_2O_5) and scandium (up to 0.6% Sc_2O_3). Titanium-iron oxides occur as masses of micron-scale crystals, commonly adjacent to the larger titanium oxide crystals. The mixed oxides contain up to 0.8% Sb_2O_3 , up to 1% V_2O_5 , up to 2.5% As_2O_3 and up to 2% P_2O_5 (Table 3). By contrast, titanium-iron oxide crystals in the andesite do not contain measurable trace elements.

Pyrite is common in the plant-bearing chert. It occurs as framboids and cubes, and intermixtures of the two (Figure 6). They consistently occur together, implying that they were coprecipitated or the cubes are a local recrystallization of the framboids. Their precipitation was very early, before the sediment was sealed by silicification. Electron microscopy (EDAX analysis) and LA-ICP-MS mapping show that the pyrite contains traces of arsenic and gold throughout (Figure 7). The gold content of the pyrite is approximately 1.2 ppm. Arsenic occurs in both the framboids (mean $0.61 \pm 0.37\%$, $n = 18$) and cubes (mean $0.55 \pm 0.54\%$, $n = 20$). Rarely, pyrite framboids also occur in the phytodebris layers, but there they are manganous (up to 1.3% Mn) (Figure 6c). LA-ICP-MS mapping of gold-bearing pyrite showed no tellurium, that is, the gold is not present as a telluride as commonly found elsewhere, but rather a substitute in the sulfide.

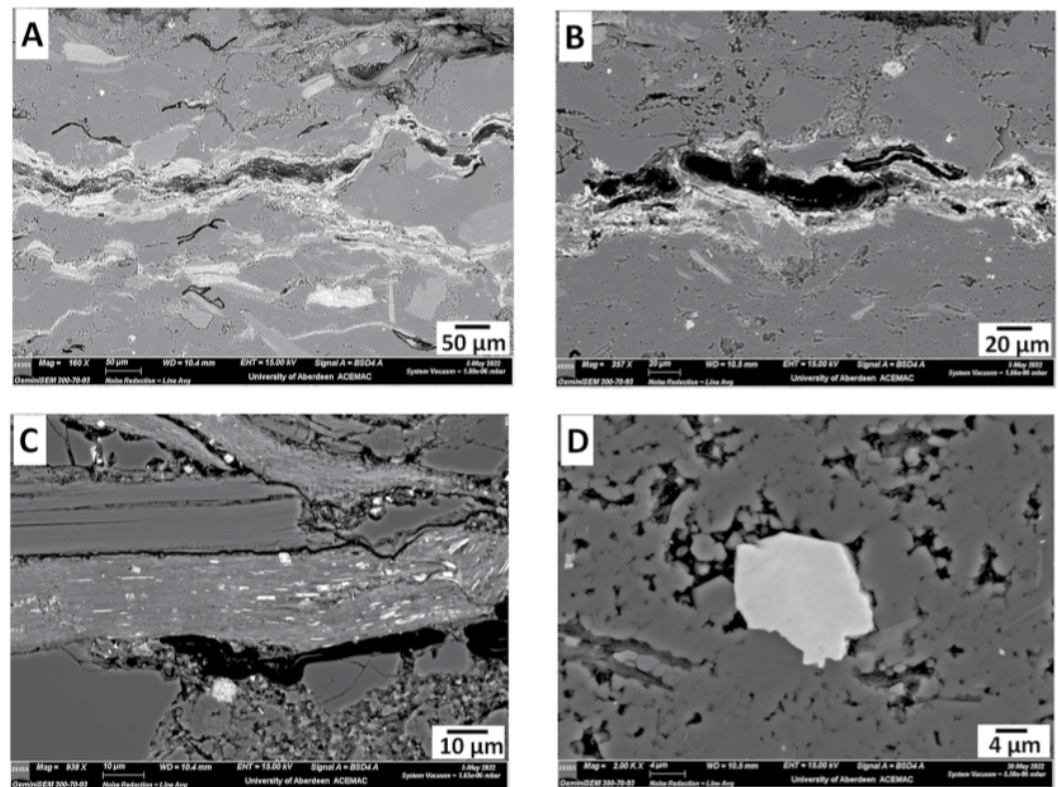


Figure 4. Backscattered scanning electron micrographs of mineral phases in phytodebris layers in Rhynie Chert. (a) Layer of carbonaceous plant fragments (black), accompanied by manganese-iron oxides (bright) and background mineralogy dominated by quartz and micas; (b) Close-up of layer of carbonaceous plant fragments (black) and manganese-iron oxides (bright); (c) Chlorite containing abundant sub-micron inclusions of manganese-iron oxides (bright), sandwiched between mica and quartz. Note pyrite framboid in lower center. (d) Tungsten-rich titanium oxide crystal, within microcrystalline quartz.

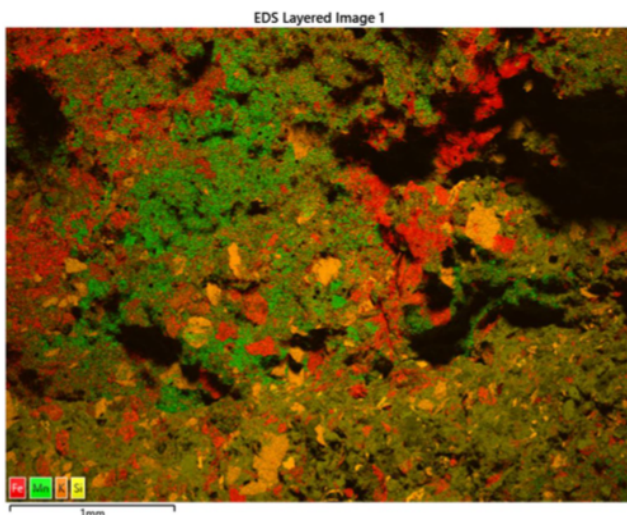


Figure 5. Layered image of element maps for Fe, Mn, K, and Si. Shows regions rich in Fe (red, iron oxide), Mn (green, manganese oxide) and Fe-Mn mixtures, Si (detrital quartz), K (detrital mica) and carbonaceous matter (black), phytodebris layer parallel to layering, Rhynie Chert.

Mixed framboidal/cubic pyrite sampled from depth ~6.3 m in trench 03/T1 yielded 5 sulfur isotope compositions ($\delta^{34}\text{S}_{\text{CDT}}$) of -0.5 , 0.0 , 0.1 , 2.1 , and 2.3‰ (mean 0.8‰). The maximum uncertainty in measurement was about 0.05‰ . Previous data (Rice et al., 1995) was recorded from the mineralized fault zone (-2.8 to $+7.3\text{‰}$) and in background shales (-23.3‰). The reproducibility of $\delta^{34}\text{S}_{\text{CDT}}$ values was evaluated through repeated analysis of standards NBS-123 ($+17.1\text{‰}$), IAEA-S-3 (-32.3‰), and a SUERC internal standard CP-1 (-4.6‰), and was typically within $\pm 0.3\text{‰}$.

The mean values of total organic carbon (TOC) measured in samples of plant-bearing chert and beds of phytodebris were $0.36 \pm 0.29\%$ ($n = 26$) and $0.77 \pm 0.35\%$ ($n = 22$) respectively.

The mean values of degree of pyritization (DOP) measured in samples of plant-bearing chert and beds of phytodebris were 39.5 ($n = 5$) and 12.7 ($n = 7$) respectively.

5. Discussion

The geochemical data provide insights into the residence of trace elements introduced into the plant-bearing sediments at Rhynie from hot spring waters and detrital grains (Figure 9, Table 4). The redox conditions help to understand the variability in the sediment section.

Table 1
Representative Analyses (%) of Manganese-Iron Oxide Precipitates in Fungus-Rich Phytodebris Layers, Rhynie Chert

Lab no.	491-1-5	491-1-4	491-2-8	491-2-6	492-9-3	492-9-2	492-8-5	492-4-1
MgO	0.3	0.4	0.0	0.3	0.3	1.2	0.2	0.3
Al ₂ O ₃	21.1	22.0	8.5	6.4	7.7	10.1	4.8	5.1
SiO ₂	4.4	8.3	2.2	4.5	6.8	12.9	4.7	5.3
P ₂ O ₅	1.1	1.1	0.9	1.1	1.6	1.6	1.6	1.6
SO ₃	0.6	0.7	0.6	0.6	0.6	0.6	1.1	1.1
K ₂ O	0.3	0.3	0.0	0.1	0.2	0.6	0.0	0.0
CaO	1.5	1.3	1.9	1.4	0.6	0.4	0.4	0.3
TiO ₂	0.0	0.2	0.0	0.0	0.3	0.3	0.0	0.0
MnO ₂	40.2	37.7	17.8	7.2	1.9	0.8	0.0	0.0
FeO ₂	10.4	11.3	45.2	56.7	77.4	70.8	82.5	82.2
As ₂ O ₃	0.4	0.4	0.9	0.8	0.0	0.0	0.0	0.0
Total	80.4	83.7	78.1	79.1	97.2	99.1	95.4	95.8

Note. Fe and Mn calculated as FeO₂ and MnO₂ as typical in soil precipitates.

5.1. The Redox Profile

The degree of pyritization can be high in soils that are rich in organic matter (Rabenhorst et al., 2020). The DOP might be expected to be greater in the layers of phytodebris, as the phytodebris has over double the content of TOC (0.77%, $n = 22$) in the plant-bearing chert (0.36%, $n = 26$). Rather, the mean DOP value for the phytodebris layers is lower (12.7) than in the plant-rich cherts (39.5). This reflects a difference in iron mineralogy (Figure 8). While the plant layers contain abundant framboids of the sulfide pyrite, the phytodebris layers contain oxides of iron, manganese and titanium. Fungi were probably an important control on oxide formation. The fungal oxidation of iron minerals produces high proportions of Fe (III) oxides and hydroxides (Bonneville et al., 2016; Oggerin et al., 2016). Similarly, fungi cause the oxidation of manganese in an otherwise reduced soil (Thompson et al., 2005).

Where pyrite framboids occur in the phytodebris layers, the pyrite is widely oxidized. Framboids in the phytodebris are manganese-bearing, which is relatively uncommon, but may reflect a high availability of manganese during their formation. Manganese-reducing fungi are unknown, so the framboids were probably a bacterial product. Oxidation has left the framboids in a matrix of jarosite (Figure 6c). Jarosite can be formed by the fungal oxidation of sulfides (Oggerin et al., 2014), and specifically the oxidation of manganese-bearing pyrite by fungi

Table 2
Representative Analyses (%) of Titanium Oxide Precipitates in Fungus-Rich Phytodebris Layers, Rhynie Chert

Lab no.	493-11-1	493-11-2	493-11-3	493-11-4	493-23-1	493-12-1	493-12-2	496-24-1	496-24-3	496-24-5
Al ₂ O ₃	0.9	1.0	0.7	0.8	0.0	0.1	0.3	0.8	0.8	1.0
SiO ₂	0.5	0.5	0.0	0.5	0.2	0.4	0.5	0.2	0.4	1.7
Sc ₂ O ₃	0.4	0.3	0.6	0.4	0.0	0.0	0.0	0.2	0.2	0.2
TiO ₂	88.7	90.5	89.2	88.7	95.9	92.8	91.3	89.7	90.2	88.0
FeO ₂	1.7	1.1	1.2	0.8	0.5	0.7	1.1	2.1	2.3	2.5
ZrO ₂	0.5	0.4	0.5	0.0	0.0	0.0	0.0	0.5	0.4	0.4
Nb ₂ O ₅	0.0	0.0	0.0	0.0	1.5	0.9	1.5	0.0	0.0	0.0
WO ₃	3.5	2.8	4.6	3.9	0.0	0.7	1.0	7.1	6.7	6.8
Total	96.1	96.4	96.7	95.1	98.1	95.6	95.6	100.6	101.0	100.5

Note. Fe calculated as FeO₂ as typical in soil precipitates.

Table 3
Representative Analyses (%) of Titanium-Iron Oxide Precipitates in Fungus-Rich Phytodebris Layers, Rhynie Chert

Lab no.	493-29-2	493-29-3	493-24-1	493-24-3	493-2-1	493-2-2	493-2-3	493-8-2	493-8-3	493-18-1	493-18-2
Al ₂ O ₃	4.3	4.4	5.1	5.1	3.9	4.6	4.2	3.3	3.4	1.4	1.6
SiO ₂	1.6	1.8	2.0	1.4	0.7	0.8	0.9	2.5	1.7	0.7	1.9
P ₂ O ₅	1.0	1.0	1.6	1.5	1.0	1.2	1.1	0.7	0.8	0.2	0.2
SO ₃	0.4	0.3	0.2	0.6	0.3	0.3	0.3	0.0	0.0	0.0	0.2
CaO	0.3	0.2	0.3	0.5	0.2	0.2	0.2	0.2	0.2	0.0	0.2
TiO ₂	47.2	45.5	47.8	44.7	38.7	33.8	36.7	57.4	56.7	84.2	82.0
V ₂ O ₅	0.5	0.5	0.5	0.6	0.7	0.6	0.5	0.5	0.5	0.9	0.7
FeO ₂	33.6	35.6	34.3	32.7	39.6	44.7	41.5	25.4	23.7	8.8	9.6
As ₂ O ₃	1.7	1.5	0.7	0.8	1.6	1.7	1.6	1.1	1.2	0.5	0.6
Sb ₂ O ₃	0.0	0.0	0.0	0.0	0.5	0.5	0.6	0.3	0.3	0.0	0.0
WO ₃	0.6	0.6	0.5	0.4	0.4	0.6	0.4	0.5	0.6	0.8	0.8
Total	91.3	91.3	93.1	88.3	87.6	88.9	87.9	91.8	89.0	97.4	97.8

Note. Fe calculated as FeO₂ as typical in soil precipitates.

has been implicated by experiment (Kruse et al., 2021). The jarosite formation from pyrite at Rhynie is consistent with a putative fungal origin for oxidation in the phytodebris layers.

The absence of red beds indicates insufficient time for normal atmospheric oxidation of the sediment at/near the surface. Nevertheless, oxides were precipitated in the phytodebris layers, and had a major control on the content of elements, as evidenced below (Table 4). The anomalous degree of oxidation in the carbonaceous phytodebris, rather than sulfide formation, is consistent with modern mycorrhizal fungi in symbiosis with local vegetation which are capable of sulfide oxidation/dissolution and bioaccumulation of metals (Cecchi et al., 2019).

5.2. Phosphorus Cycling

The dissolution of monazite grains is important as a source of phosphorus. The monazite was dissolved more extensively than other minerals. At Rhynie, where the sediment was pervasively colonized by fungi which required phosphorus to deliver to the plants, the fungi are implicated as the cause of dissolution. The dissolution of monazite by fungi is well documented in soil and laboratory (Brisson et al., 2016; Castro et al., 2020; Corbett et al., 2017; Fathollahzadeh et al., 2019; Kang et al., 2021). Bioweathering by fungi leaves monazite grains porous and with elaborate crystal architecture (Figure 2d of Kang et al., 2021). The architecture of monazite grains in the Rhynie Chert (Figure 3) matches those of grains known to be fungally bioweathered, so this origin is concluded at Rhynie. Biologically mediated weathering has been suggested at Rhynie based on limited sculpture on quartz/feldspar grain surfaces (Mitchell et al., 2016, 2019), but the alteration of monazite reported here is to a much greater extent. In addition to the immediately available phosphorus in the fungi-bearing phytodebris layers, phosphorus could have been supplied from monazite in the nearby granite. However, monazite in both the granite, and plant-free sandstone below the Rhynie Chert, do not exhibit the porous alteration developed in monazite within the Rhynie Chert sand. The monazite in the chert is distinctive, which suggests bioweathering.

Manganese-iron oxides are also a common product of fungal activity. Manganese is an essential nutrient for plants, like phosphorus, and the uptake of both manganese and iron is important to the mycorrhizal symbiosis (Marschner, 1995). Fungi can readily solubilize and redeposit manganese oxides (Garcia et al., 2020; Santelli et al., 2011), which explains the concentration of oxides in the phytodebris layers. Mn oxides in soil have a high capacity to adsorb trace elements including phosphorus and arsenic (Huang, 1991; Suda & Makino, 2016). This includes fungally precipitated Mn-Fe oxides (Owoccki et al., 2016), as occurs at Rhynie. Thus, the oxides at Rhynie may have acted as an intermediate reservoir of phosphorus that the fungi could access when required.

Pertinent to Rhynie, manganese oxides are formed by fungi in hot spring environments (Ferris et al., 1987; Mita & Miura, 2003). An anomalous manganese content in the mineralized Rhynie Fault Zone (Rice & Trewin, 1988) shows that there was a ready supply to the plant-colonized sediments where fungal mineralization could contribute

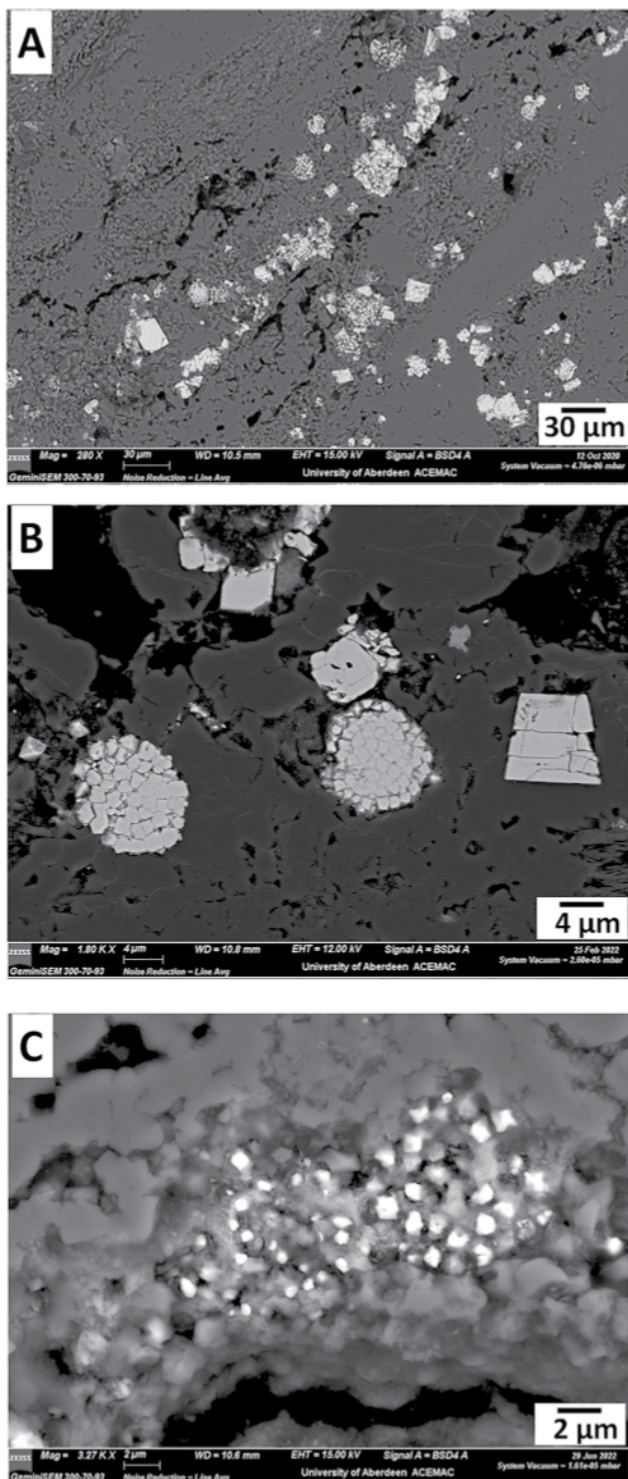


Figure 6. Backscattered scanning electron micrographs of pyrite in Rhynie Chert. (a) Mixed framboids and cubic pyrite (bright), adjacent to carbonaceous plant matter (black) in quartzose matrix. Framboids are arsenic-bearing; (b) Pyrite framboids in quartz; (c) Oxidation of manganese-bearing pyrite, in which remnant pyrite (bright) occurs in matrix of jarosite (light gray), in quartzose matrix.

to the precipitation of the oxides. Coeval manganese ore deposits in the same region (Nicholson, 1986, 1989) were a further supply of both manganese and antimony. As the oxides stored phosphorus, manganese was central to the plant-fungal symbiosis at Rhynie. Manganese was also incorporated in the pyrite framboids in the phytodebris layers.

5.3. Arsenic, Tungsten, and Antimony

The arsenic and gold in pyrite within the Rhynie Chert shows that the trace elements introduced by the hydrothermal system were present in the plant habitat. They also show that the pyrite was effective in removing and immobilizing these elements. Framboid formation at the near-surface was probably a product of bacteria (Wacey et al., 2015). Arsenic is toxic to plant growth, especially in the As (III) form that would have been engendered by the organic-rich environment (Liu et al., 2006). Microbial sulfate reduction to precipitate As-bearing pyrite (Fischer et al., 2021; Gao et al., 2021) meant that a bacterial component made the groundwater less toxic to plants, which would have reduced stress on the whole ecosystem. Notably, arsenian pyrite formed in an organic-rich medium includes mixed framboids and euhedra (Fischer et al., 2021), as found at Rhynie. Arsenian pyrite is a common residence for gold in low-temperature rocks (Reich et al., 2005), so indirectly the concentration of gold can be microbially mediated. In addition, an essential aspect of symbiosis is the reduction of arsenic uptake into plants by associated arbuscular mycorrhizal fungi (Li et al., 2021; Neidhardt, 2020; Zhang et al., 2015). The manganese oxides can also oxidize As(III) to the less toxic, and less mobile, As(V) (Huang, 1991; Suda & Makino, 2016).

Pyrite is common in the chert (Trewin & Fayers, 2015; Wellman, 2006). In a setting that has a high sedimentation rate (Powell et al., 2000), characteristic of continental successions, the pyrite represents an abundant input of sulfur. The hot spring system is the obvious source of abundant sulfur, which was being continually renewed during the lifetime of the system. The sulfur isotope data helps to demonstrate that this was so. A hot spring source is borne out by the similarity of $\delta^{34}\text{S}_{\text{CDT}}$ values for the pyrite in the chert (mean 0.8‰) and the mineralized fault zone (−2.8 to +7.3‰, from Rice et al. [1995]). These data are in contrast to the light composition of sulfur in pyrite deposited in background shales (−23.3‰, Rice et al., 1995), reflecting microbial sulfate reduction in lake waters.

Arsenic and phosphorus biochemistry in plants are linked, and the two elements may be co-transported (Zhao et al., 2009). Mycorrhizal plants commonly have a relatively high ratio of P/As concentration, which is likely to increase tolerance of the plant to As (Zhao et al., 2009). Phosphate causes plant tolerance to As through a number of mechanisms (Abbas et al., 2018), so together with the effects of manganese oxide and pyrite there are multiple ways in which arsenic stress may have been alleviated at Rhynie.

The titanium oxide crystals have up to 8% WO_3 , and they may have removed that element from the ecosystem. The crystals additionally contain up to 2% Nb_2O_5 and 0.6% Sc_2O_3 (Table 2). The combination of crystalline shape and trace element content indicates that the titanium oxide mineral is rutile. Mixed iron-titanium oxides at Rhynie also contain traces of Sb_2O_3 , V_2O_5 , As_2O_3 , and P_2O_5 (Table 3). Tungsten, niobium, scandium and antimony can all be enriched within rutile (Černý & Chapman, 2001). Titanium oxides are a primary scavenger and carrier of tungsten in low-temperature sedimentary rocks (Majzlan et al., 2021), and iron oxides are well known to adsorb

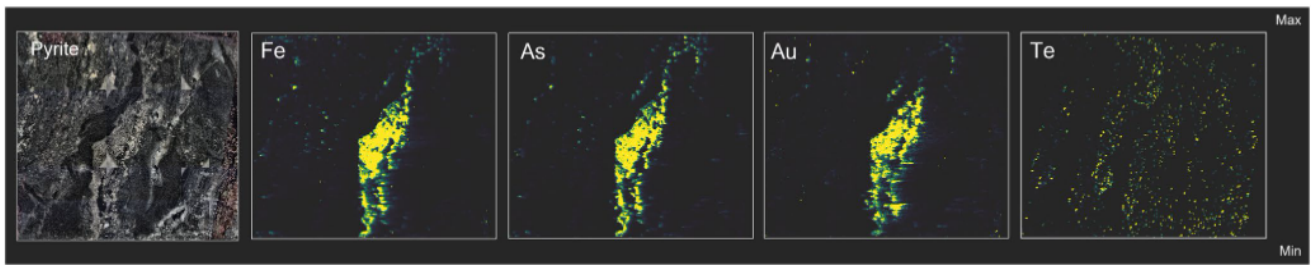


Figure 7. Element maps (Fe, As, Au, Te) for pyrite in Rhynie Chert. Determined by LA-ICP-MS (conditions in text). Arsenic and gold are trace substitutes in the sulfide. Absence of tellurium shows gold is not a telluride. Maps each width 5 mm.

antimony in soils (Shangguan et al., 2016). The mineral residence of tungsten and antimony at Rhynie therefore follows their expected distribution. Titanium oxide is concentrated by common fungi (at present *Aspergillus niger*, found in hot springs) in soils (Šebesta et al., 2020), and this fungus can also solubilize both tungsten (Pattanaik et al., 2022) and antimony (Milová-Žiaková et al., 2016), so they may be linked in a single process. Arbuscular mycorrhizal fungi can also reduce the antimony toxicity to plants (Pierart et al., 2017), and similar activity could have occurred in the fungi-bearing soils at Rhynie. Notably, the titanium-iron oxides in the andesite, formed at a high temperature and where no fungi were present, do not contain the trace elements. The niobium is most likely derived from granitic basement, as niobium-bearing tungsten mineralization occurs in granite/pegmatite (Shaw & Goodenough, 2013; Smith et al., 2019) and niobium-rich stream sediments are derived from granite (Beer & Bennett, 1988) in the same region. Limited data indicate niobium toxicity to plants at high concentrations (Paquet et al., 2019). Vanadium is similarly toxic to plants at high concentrations, although beneficial at moderate concentrations (Larsson et al., 2013). Scandium had not been measured previously at Rhynie, but it does occur in hot spring systems (Hoshina et al., 2014; Simmons et al., 2018). Like several other trace elements, scandium (Qu et al., 2015; Syrvatka et al., 2022) and vanadium (Rasoulnia & Mousavi, 2016) can be mobilized by *Aspergillus niger*.

5.4. Timescale and Trace Element Flux

The incorporation of plants in growth position by silicification events at Rhynie implies that the timescale was limited, although plant-bearing beds are separated by layers of compacted phytodebris (Figure 8). Analogous preservation of plants by opal at Yellowstone National Park takes place on a month-to-year timescale (Channing & Edwards, 2004). Recognizable soil profiles did not have enough time to develop in the Rhynie sediments before silicification, so sedimentation rates were likely to be in the range of mm/a to cm/a (Channing, 2017; Powell et al., 2000; Trewin & Fayers, 2015). Previous studies show that substantial element liberation from fungally colonized monazite can occur within days (Brisson et al., 2016; Castro et al., 2020; Kang et al., 2021). The very rapid processing of monazite grains implies that even where local sedimentation rates are high, new grains

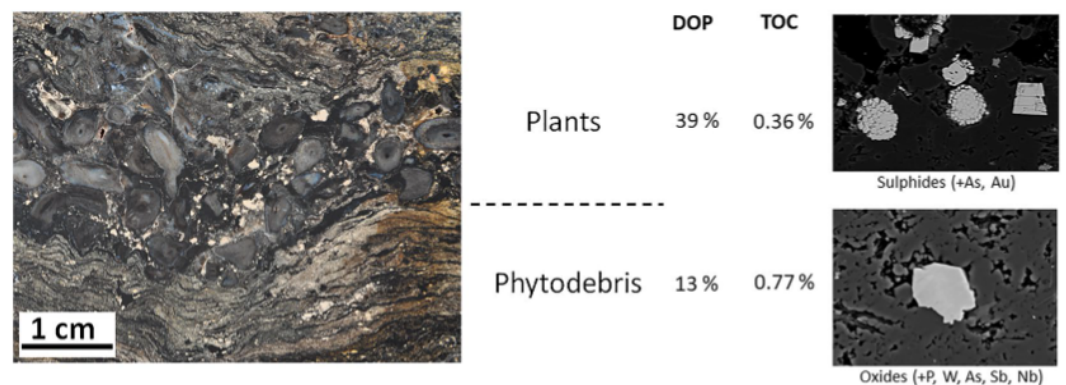


Figure 8. Contrast between plant-bearing chert and layers of phytodebris. Phytodebris layers have more total organic carbon (TOC), but lower degree of pyritization (DOP). Greater oxide formation in these layers implies fungal activity, which overrides normal redox characteristics. Oxides and sulfides (pyrite) sequester different trace elements.

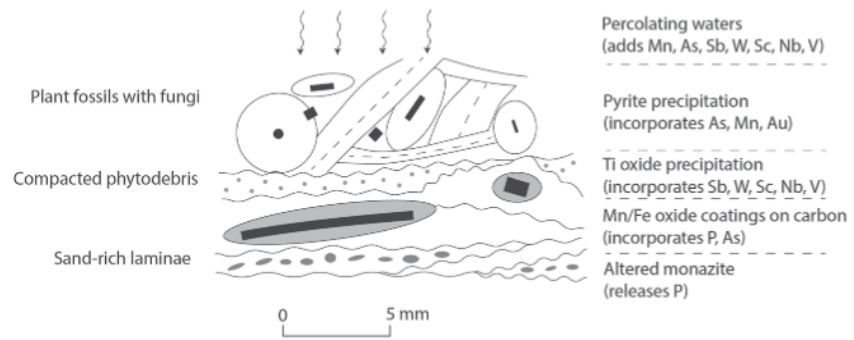


Figure 9. Schematic section of plant-bearing chert upon sediment rich in phytodebris and detrital grains. Incoming trace elements from percolating hot spring waters and altered detrital grains were precipitated in oxides and sulfides.

are likely to be altered by fungi within the uppermost few centimeters of sediment. Similarly, fungi precipitate manganese oxides during growth (Thompson et al., 2005), and sulfate-reducing bacteria can precipitate arsenian pyrite in days to weeks (Fischer et al., 2021). These data suggest that the mineral assemblage in the ecosystem would have been able to respond to incoming elements rapidly, before the system was sealed by silicification.

An assessment of the degree to which the mineral assemblage in the ecosystem had fixed trace elements is limited by uncertainties in water composition, water flow rates, regional hydrology and overall time frame. However, it is reasonable to assume an anomalous input from the spring waters. Data from hot springs in three regions considered analogous to Rhynie (Channing, 2017), Yellowstone (USA), Iceland and New Zealand, show that the content of trace elements discussed here are typically one to two orders of magnitude higher than in average river waters (Table 5). The ingress of water occurred repeatedly, as evidenced by multiple beds of plants silicified in growth position, separated by beds of phytodebris (Trewin & Fayers, 2015). Combined with high contents of trace elements in the water, this implies that there was a high flux through the sediment. The ponding implied by silicification of sediment, the subdued topography of a floodplain environment, and analogy with modern hot spring environments, all suggest that drainage was slow enough to allow precipitation of the trace elements out of solution. The chemistry of the spring waters was therefore reflected in mineral phases containing antimony, tungsten, scandium and niobium, which are rarely recorded in low-temperature (sedimentary) environments, as well as manganese, phosphorus and arsenic. It is not possible to quantify a proportion of trace elements in

Table 4
Predominant Source, Potential Role, and Mineral Residence of Trace Elements in Rhynie Chert Ecosystem

Element	Source	Role	Residence in chert	Max. content
Phosphorus	Eroded basement	Metabolism via fungi	Mn-Fe oxides	2% P ₂ O ₅
			Ti oxide	
			Residual monazite	
Tungsten	Eroded basement, Hot springs	Toxic	Ti oxide	8% WO ₃
Niobium	Eroded basement	Toxic when abundant	Ti oxide	2% Nb ₂ O ₅
Manganese	Hot springs	Metabolism via fungi	Mn-Fe oxides	50% MnO ₂
			Pyrite	1.3% Mn
Arsenic	Hot springs	Toxic	Pyrite	2.5% As
			Some metabolism	Fe-Ti oxide
Antimony	Hot springs	Toxic	Fe-Ti oxide	0.8% Sb ₂ O ₃
			Some metabolism	
Vanadium	Hot springs	Toxic when abundant	Fe-Ti oxide	1% V ₂ O ₅
Scandium	Hot springs	Inert	Ti oxide	0.6% Sc ₂ O ₃
Gold	Hot springs	Inert (Possible ore)	Pyrite	1.2 ppm Au

Table 5
Content of Trace Elements in Hot Spring Waters From Yellowstone (USA) and Iceland, Compared With Mean Global River Water Compositions

Element	Global river waters, mean (Gaillardet et al., 2003)	Iceland hot springs, range (Kaasalainen et al., 2015)	Iceland hot springs, range (Planer-Friedrich et al., 2020)	Yellowstone hot springs, range (Planer-Friedrich et al., 2020)	New Zealand Champagne Pool (Ullrich et al., 2013)
Mn (ppb)	34	0.13–2010			
Ti (ppb)	0.49	0.06–14.9			
As (ppb)	0.62	<0.1–162	0–78	339–4,382	4,300–8,480
Sb (ppb)	0.07	0.01–23	0.3–5.4	2–161	6–542
W (ppb)	0.1	0.1–70.6	0–20.5	0.6–407.7	54–162
V (ppb)	0.71	0.08–22.9			

the water fixed by the minerals, but it can be inferred that the oxide and sulfide phases which incorporate them included biological precipitates, and hence the ecosystem accounted for a high proportion of their precipitation.

5.5. Fungi and Heavy Metals

Mycoremediation, to extract heavy metals and other pollutants, has become an established approach to environmental clean-up (Kumar & Dwivedi, 2021), including using arbuscular mycorrhizae (Cabral et al., 2015; Göhre & Paszkowski, 2006; Meyer et al., 2017; Riaz et al., 2021). This implies that fungi have evolved with this capability. Sheldrake (2019) argues that “fungi are some of the best qualified organisms for environmental remediation....fine-tuned over a billion years of evolution.” Exposure to metals is believed to have driven the progressive evolution of metal tolerance in fungi (Colpaert et al., 2011). Arbuscular mycorrhizae and other fungi in metal-contaminated environments can develop resistance within a few years (Sudová et al., 2007; Tullio et al., 2003). The Lower Devonian succession at Rhynie was deposited in gradual onlap of Ordovician serpentinite and chromite-bearing rocks (Busrewil et al., 1973), as evidenced by detrital chromite in the Rhynie Chert, so the ambient fungal community may have been pre-conditioned to heavy metal tolerance. We do not know, however, how the tolerance to trace elements in Devonian plants compared to that in modern plants. Genomic evidence indicates a fungal response to heavy metals deep in geological time (Chi et al., 2021). The precipitation of minerals that sequestered metals at Rhynie, as opposed to tolerance of metal build-up in the biomass, may have been an early expression of that capability.

6. Conclusions

Petrographic and geochemical studies of mineral phases in the Rhynie Chert show how elements contributed by a combination of hydrothermal activity and detrital sediment were accommodated by the ecosystem (Table 4). In particular:

1. Grains of monazite in the sediment were extensively altered, likely by fungi, to release phosphorus into the ecosystem.
2. Phosphorus was stored in the ecosystem in manganese-iron oxide precipitates, and titanium oxides.
3. Tungsten and niobium from granites supplying the sediment to the ecosystem was sequestered into titanium oxides.
4. Antimony, vanadium and scandium from the hot spring system were also incorporated into titanium oxides.
5. Arsenic from the hot spring system was incorporated into widespread pyrite precipitated by bacteria, and also in the oxide precipitates.
6. Gold was also incorporated into the pyrite, thus incidentally controlled by bacteria.

In summary, the mineral assemblage at Rhynie controlled the trace element geochemistry of the ambient waters.

Conflict of Interest

The authors declare no conflicts of interest relevant to this study.

Data Availability Statement

Data reported in Tables 1–3 is managed by the University of Aberdeen (<https://doi.org/10.20392/eed913d7-12eb-4c5d-a276-e1920eecd43f>).

Acknowledgments

JGTA is supported by the Natural Environment Research Council (Grant NE/T003677/1). Samples were archived at the University of Aberdeen by N.H. Trewin, S.R. Fayers, and C.M. Rice. Skilled technical support was provided by J. Johnston, J. Bowie, W. Ritchie, and C. Taylor. We are grateful for the comments of two reviewers which improved the manuscript.

References

- Abbas, G., Murtaza, B., Bibi, I., Shahid, M., Niazi, N. K., Khan, M. I., et al. (2018). Arsenic uptake, toxicity, detoxification, and speciation in plants: Physiological, biochemical and molecular aspects. *International Journal of Environmental Research and Public Earth*, *15*(1), 59. <https://doi.org/10.3390/ijerph15010059>
- Adamakis, I. D., Panteris, E., & Eleftheriou, E. P. (2012). Tungsten toxicity in plants. *Plants*, *1*(2), 82–99. <https://doi.org/10.3390/plants1020082>
- Baron, M., Hillier, S., Rice, C. M., Czapnik, K., & Parnell, J. (2004). Fluids and hydrothermal alteration assemblages in a Devonian gold-bearing hot-spring system, Rhynie, Scotland. *Transactions of the Royal Society of Edinburgh Earth Sciences*, *94*(4), 309–324. <https://doi.org/10.1017/s0263593300000717>
- Beer, K. E., & Bennett, M. J. (1988). Geochemistry of sediments from the Lui drainage, Braemar, Grampian. *British Geological Survey Mineral Reconnaissance Programme, Report No. 96*.
- Bonneville, S., Andrew, A. W., & Benning, L. G. (2016). Structural Fe(II) oxidation in biotite by an ectomycorrhizal fungi drives mechanical forcing. *Environmental Science and Technology*, *50*(11), 5589–5596. <https://doi.org/10.1021/acs.est.5b06178>
- Brisson, V. L., Zhuang, W. Q., & Alvarez-Cohen, L. (2016). Bioremediation of rare Earth elements from monazite sand. *Biotechnology and Bioengineering*, *113*(2), 339–348. <https://doi.org/10.1002/bit.25823>
- Brundrett, M. C., Walker, C., Harper, C. J., & Krings, M. (2018). *Fossils of arbuscular mycorrhizal fungi give insights into the history of a successful partnership with plants. Transformative Paleobotany: Papers to Commemorate the Life and Legacy of Thomas N. Taylor* (pp. 461–480). Academic Press.
- Burghlea, C., Zaharescu, D. G., Dontsova, K., Maier, R., Huxman, T., & Chorover, J. (2015). Mineral nutrient mobilization by plants from rock: Influence of rock type and arbuscular mycorrhiza. *Biogeochemistry*, *124*(1–3), 187–203. <https://doi.org/10.1007/s10533-015-0092-5>
- Buswail, M. T., Pankhurst, R. J., & Wadsworth, W. J. (1973). The igneous rocks of the Bogancloch area, N.E. Scotland. *Scottish Journal of Geology*, *9*(3), 165–176. <https://doi.org/10.1144/sjg09030165>
- Cabral, L., Soares, C. R. F., Giachini, A. J., & Siqueira, J. O. (2015). Arbuscular mycorrhizal fungi in phytoremediation of contaminated areas by trace elements: Mechanisms and major benefits of their applications. *World Journal of Microbiology and Biotechnology*, *31*(11), 1655–1664. <https://doi.org/10.1007/s11274-015-1918-y>
- Castro, L., Blázquez, M. L., González, F., & Muñoz, J. A. (2020). Bioremediation of phosphate minerals using *Aspergillus niger*: Recovery of copper and rare Earth elements. *Metals*, *10*(7), 978. <https://doi.org/10.3390/met10070978>
- Cecchi, G., Di Piazza, S., Marescotti, P., & Zotti, M. (2019). Evidence of pyrite dissolution by *Telephora terrestris* Ehrh in the Libiola mine (Sestri Levante, Liguria, Italy). *Heliyon*, *5*(8), e02210. <https://doi.org/10.1016/j.heliyon.2019.e02210>
- Černý, P., & Chapman, R. (2001). Exsolution and breakdown of Scandian and tungstenian Nb-Ta-Ti-Fe-Mn phases in niobian rutile. *The Canadian Mineralogist*, *39*(1), 93–101. <https://doi.org/10.2113/gscanmin.39.1.93>
- Channing, A. (2017). A review of active hot-spring analogues of Rhynie: Environments, habitats and ecosystems. *Philosophical Transactions of the Royal Society*, *B373*(1739), 20160490. <https://doi.org/10.1098/rstb.2016.0490>
- Channing, A., & Edwards, D. (2004). Experimental taphonomy: Silicification of plants in Yellowstone hot spring environments. *Transactions of the Royal Society of Edinburgh Earth Sciences*, *94*(4), 503–521. <https://doi.org/10.1017/s0263593300000845>
- Channing, A., & Edwards, D. (2009). Yellowstone hot spring environments and the palaeo-ecophysiology of Rhynie chert plants: Towards a synthesis. *Plant Ecology & Diversity*, *2*, 111–143. <https://doi.org/10.1080/17550870903349359>
- Chi, B., Lu, Y., Yin, P., Liu, H., Chen, H., & Shan, Y. (2021). Sequencing and comparative genomic analysis of a highly metal-tolerant *Penicillium janthinellum* P1 provide insights into its metal tolerance. *Frontiers in Microbiology*, *12*, 663217. <https://doi.org/10.3389/fmicb.2021.663217>
- Colpaert, J. V., Wevers, J. H. L., Krznaric, E., & Adriaenssen, K. (2011). Heavy metal-tolerant ecotypes of ectomycorrhizal fungi protect plants from heavy metal pollution. *Annals of Forest Science*, *68*(1), 17–24. <https://doi.org/10.1007/s13595-010-0003-9>
- Corbett, M. K., Eksteen, J. J., Niu, X.-Z., Croue, J.-P., & Watkin, E. L. (2017). Interactions of phosphate solubilising microorganisms with natural rare-Earth phosphate minerals: A study utilizing Western Australian monazite. *Bioprocess and Biosystems Engineering*, *40*(6), 929–942. <https://doi.org/10.1007/s00449-017-1757-3>
- Fathollahzadeh, H., Eksteen, J. J., Kaksonen, A. H., & Watkin, E. L. J. (2019). Role of microorganisms in bioremediation of rare Earth elements from primary and secondary resources. *Applied Microbiology and Biotechnology*, *103*(3), 1043–1057. <https://doi.org/10.1007/s00253-018-9526-z>
- Ferris, F. G., Fyfe, W. S., & Beveridge, T. J. (1987). Manganese oxide deposition in a hot spring microbial mat. *Geomicrobiology Journal*, *5*(1), 33–42. <https://doi.org/10.1080/01490458709385955>
- Fischer, A., Saunders, J., Speetjens, S., Marks, J., Redwine, J., Rogers, S. R., et al. (2021). Long-term arsenic sequestration in biogenic pyrite from contaminated groundwater: Insights from field and laboratory studies. *Minerals*, *11*(5), 537. <https://doi.org/10.3390/min11050537>
- Gaillardet, J., Viers, J., & Dupré, B. (2003). Trace elements in river waters. In J. I. Drever (Ed.), *Treatise on Geochemistry, Surface and Groundwater, Weathering and Soils* (pp. 225–272). Elsevier.
- Gao, J., Zheng, T., Deng, Y., & Jiang, H. (2021). Microbially mediated mobilization of arsenic from aquifer sediments under bacterial sulfate reduction. *Science of The Total Environment*, *768*, 144709. <https://doi.org/10.1016/j.scitotenv.2020.144709>
- Garcia, K. G. V., Mendes Filho, P. F., Pinheiro, J. I., do Carmo, J. F., de Araújo Pereira, A. P., Martins, C. M., et al. (2020). Attenuation of manganese-induced toxicity in *Leucaena leucocephala* colonized by arbuscular mycorrhizae. *Water Air and Soil Pollution*, *231*(1), 22. <https://doi.org/10.1007/s11270-019-4381-9>
- George, E., Marschner, H., & Jakobsen, I. (1995). Role of arbuscular mycorrhizal fungi in uptake of phosphorus and nitrogen from soil. *Critical Reviews in Biotechnology*, *15*(3–4), 257–270. <https://doi.org/10.3109/07388559509147412>

- Göhre, V., & Paszkowski, U. (2006). Contribution of the arbuscular mycorrhizal symbiosis to heavy metal phytoremediation. *Planta*, 223(6), 1115–1122. <https://doi.org/10.1007/s00425-006-0225-0>
- Harper, C. J., Walker, C., Schwendemann, A. B., Kerp, H., & Krings, M. (2020). *Archaeosporites rhyniensis* gen. et sp. nov. (Glomeromycota, Archaeosporaceae) from the Lower Devonian Rhynie chert: A fungal lineage morphologically unchanged for more than 400 million years. *Annals of Botany*, 126(5), 915–928. <https://doi.org/10.1093/aob/mcaa113>
- Hildebrandt, U., Regvar, M., & Bothe, H. (2007). Arbuscular mycorrhiza and heavy metal tolerance. *Phytochemistry*, 68(1), 139–146. <https://doi.org/10.1016/j.phytochem.2006.09.023>
- Hoshina, H., Kasai, N., Amada, H., Seko, N., Takahashi, M., & Tanaka, K. (2014). Recovery of scandium from hot spring water with graft adsorbent containing phosphoric groups. *Nippon Ion Kokan Gakkai-Shi*, 25(4), 248–251. <https://doi.org/10.5182/jaie.25.248>
- Huang, P. M. (1991). Kinetics of redox reactions on manganese oxides and its impact on environmental quality. *Rates of Soil Chemical Processes*, 27, 191–230. <https://doi.org/10.2136/sssaspecpub27.c8>
- Kaasalainen, H., Stefánsson, A., Giroud, N., & Arnórsson, S. (2015). The geochemistry of trace elements in geothermal fluids, Iceland. *Applied Geochemistry*, 62, 207–223. <https://doi.org/10.1016/j.apgeochem.2015.02.003>
- Kang, X., Csetenyi, L., & Gadd, G. M. (2021). Colonization and bioweathering of monazite by *Aspergillus niger*: Solubilization and precipitation of rare Earth elements. *Environmental Microbiology*, 23(7), 3970–3986. <https://doi.org/10.1111/1462-2920.15402>
- Krings, M., Harper, C. J., & Taylor, E. L. (2018). Fungi and fungal interactions in the Rhynie chert: A review of the evidence, with the description of *Perexiflasca tayloriana* gen. et sp. nov. *Philosophical Transactions of the Royal Society B*, 373(1739), 20160500. <https://doi.org/10.1098/rstb.2016.0500>
- Kruse, S., Rosenfeld, C., & Herndon, E. (2021). Manganese uptake by red maples in response to mineral dissolution rates in soil. *Biogeochemistry*, 155(2), 147–168. <https://doi.org/10.1007/s10533-021-00817-4>
- Kumar, V., & Dwivedi, S. K. (2021). Mycoremediation of heavy metals: Processes, mechanisms, and affecting factors. *Environmental Science and Pollution Research*, 28(9), 10375–10412. <https://doi.org/10.1007/s11356-020-11491-8>
- Larsson, M. A., Baken, S., Gustafsson, J. P., Hadialhejazi, G., & Smolders, E. (2013). Vanadium bioavailability and toxicity to soil microorganisms and plants. *Environmental Toxicology and Chemistry*, 32(10), 2266–2273. <https://doi.org/10.1002/etc.2322>
- Leventhal, J., & Taylor, C. (1990). Comparison of methods to determine degree of pyritization. *Geochimica et Cosmochimica Acta*, 54(9), 2621–2625. [https://doi.org/10.1016/0016-7037\(90\)90249-k](https://doi.org/10.1016/0016-7037(90)90249-k)
- Li, J., Chen, B., Zhang, X., Hao, Z., Zhang, X., & Zhu, Y. (2021). Arsenic transformation and volatilization by arbuscular mycorrhizal symbiosis under axenic conditions. *Journal of Hazardous Materials*, 413, 125390. <https://doi.org/10.1016/j.jhazmat.2021.125390>
- Liu, G. J., Zhang, X. R., Jain, J., Talley, J. W., & Neal, C. R. (2006). Stability of inorganic arsenic species in simulated raw waters with the presence of NOM. *Water Science and Technology: Water Supply*, 6, 175–182. <https://doi.org/10.2166/ws.2006.954>
- Majzlan, J., Bolanz, R., Göttlicher, J., Mikuš, T., Milovská, S., Čaplovičová, M., et al. (2021). Incorporation mechanism of tungsten in W-Fe-Cr-V-bearing rutile. *American Mineralogist*, 106(4), 609–619. <https://doi.org/10.2138/am-2021-7653>
- Marschner, H. (1995). *Mineral nutrition of higher plants*. Academic Press Inc.
- Meharg, A. A. (2002). Arsenic and old plants. *New Phytologist*, 156, 1–4. <https://doi.org/10.1046/j.1469-8137.2002.00513.x>
- Meharg, A. A., & Hartley-Whitaker, J. (2002). Arsenic uptake and metabolism in arsenic resistant and nonresistant plant species. *New Phytologist*, 154(1), 29–43. <https://doi.org/10.1046/j.1469-8137.2002.00363.x>
- Meyer, E., Londoño, D. M. M., de Armas, R. D., Giachini, A. J., Rossi, M. J., Stoffel, S. C. G., & Soares, C. R. F. S. (2017). Arbuscular mycorrhizal fungi in the growth and extraction of trace elements by *Chrysopogon zizanioides* (vetiver) in a substrate containing coal mine wastes. *International Journal of Phytoremediation*, 19(2), 113–120. <https://doi.org/10.1080/15226514.2016.1207596>
- Mills, B. J. W., Batterman, S. A., & Field, K. J. (2018). Nutrient acquisition by symbiotic fungi governs Palaeozoic climate transition. *Philosophical Transactions of the Royal Society B: Biological Sciences*, 373, 1739. <https://doi.org/10.1098/rstb.2016.0503>
- Milová-Žiaková, B., Urík, M., Boriová, K., Bujdoš, M., Kolenčík, M., Mikušová, P., et al. (2016). Fungal solubilization of manganese oxide and its significance for antimony mobility. *International Biodeterioration & Biodegradation*, 114, 157–163. <https://doi.org/10.1016/j.ibiod.2016.06.011>
- Mita, N., & Miura, H. (2003). Evidence of microbial activity in the formation of manganese wads at the Asahidake Hot Spring in Hokkaido, Japan. *Resource Geology*, 53(3), 233–238. <https://doi.org/10.1111/j.1751-3928.2003.tb00173.x>
- Mitchell, R. L., Cuadros, J., Duckett, J. G., Pressel, S., Mavris, C., Sykes, D., et al. (2016). Mineral weathering and soil development in the earliest land plant ecosystems. *Geology*, 44(12), 1007–1010. <https://doi.org/10.1130/g38449.1>
- Mitchell, R. L., Strullu-Derrien, C., & Kenrick, P. (2019). Biologically mediated weathering in modern cryptogamic ground covers and the early Paleozoic fossil record. *Journal of the Geological Society*, 176(3), 430–439. <https://doi.org/10.1144/jgs2018-191>
- Neidhardt, H. (2020). Arbuscular mycorrhizal fungi alleviate negative effects of arsenic-induced stress on crop plants: A meta-analysis. *Plants People Planet*, 3(5), 523–535. <https://doi.org/10.1002/ppp3.10122>
- Nicholson, K. (1986). Mineralogy and geochemistry of manganese and iron veins, Arndilly, Banffshire. *Scottish Journal of Geology*, 22(2), 213–224. <https://doi.org/10.1144/sjg22020213>
- Nicholson, K. (1989). Early Devonian geothermal systems in northeast Scotland: Exploration targets for epithermal gold. *Geology*, 17(6), 568–571. [https://doi.org/10.1130/0091-7613\(1989\)017<0568:edgsin>2.3.co;2](https://doi.org/10.1130/0091-7613(1989)017<0568:edgsin>2.3.co;2)
- Oggerin, M., Rodríguez, N., del Moral, C., & Amils, R. (2014). Fungal jarosite biomineralization in Río Tinto. *Research in Microbiology*, 165(9), 719–725. <https://doi.org/10.1016/j.resmic.2014.10.001>
- Oggerin, M., Tornos, F., Rodríguez, N., Pascual, L., & Ricardo, A. (2016). Fungal iron biomineralization in Río Tinto. *Minerals*, 6(2), 37. <https://doi.org/10.3390/min6020037>
- Owocik, K., Kremer, B., Wrzosek, B., Królikowska, A., & Kaźmierczak, J. (2016). Fungal ferromanganese mineralisation in Cretaceous dinosaur bones from the Gobi Desert, Mongolia. *PLoS One*, 11(2), e0146293. <https://doi.org/10.1371/journal.pone.0146293>
- Paquet, N., Indiketi, N., Dalencourt, C., Larivière, D., Roberge, S., Gruyer, N., et al. (2019). Toxicity of tailing leachates from a niobium mine toward three aquatic organisms. *Ecotoxicology and Environmental Safety*, 176, 355–363. <https://doi.org/10.1016/j.ecoenv.2019.03.065>
- Parry, S. F., Noble, S. R., Crowley, Q. G., & Wellman, C. H. (2011). A high-precision U–Pb age constraint on the Rhynie Chert Konservat-Lagerstätte: Time scale and other implications. *Journal of the Geological Society*, 168(4), 863–872. <https://doi.org/10.1144/0016-76492010-043>
- Pattanaik, A., Sukla, L. B., Devi, N., Pradhan, N., & Pradhan, D. (2022). Tungsten dissolution from Hutti Goldmine overburden by *Aspergillus niger*. *Geomicrobiology Journal*, 39(6), 496–501. <https://doi.org/10.1080/01490451.2022.2036878>
- Pierart, A., Dumat, C., Maes, A. Q., & Sejalón-Delmas, N. (2017). Influence of arbuscular mycorrhizal fungi on antimony phyto-uptake and compartmentation in vegetables cultivated in urban gardens. *Chemosphere*, 191, 272–279. <https://doi.org/10.1016/j.chemosphere.2017.10.058>

- Planer-Friedrich, B., Forberg, J., Lohmayer, R., Kerl, C. F., Boeing, F., Kaasalainen, H., & Stefánsson, A. (2020). Relative abundance of thiolated species of As, Mo, W, and Sb in hot springs of Yellowstone National Park and Iceland. *Environmental Science & Technology*, *54*(7), 4295–4304. <https://doi.org/10.1021/acs.est.0c00668>
- Powell, C. L., Trewin, N. H., & Edwards, D. (2000). Palaeoecology and plant succession in a borehole through the Rhynie cherts, Lower Old Red Sandstone, Scotland. In P. F. Friend & B. P. J. Williams (Eds.), *New perspectives on the Old Red Sandstone* (Vol. 180, pp. 439–457). Geological Society, London, Special Publications.
- Qu, L., Li, H., Tian, W., Wang, X., Wang, X., Jia, X., et al. (2015). Leaching of valuable metals from red mud via batch and continuous processes by using fungi. *Minerals Engineering*, *81*, 1–4. <https://doi.org/10.1016/j.mineng.2015.07.022>
- Rabenhorst, M. C., Fanning, D. S., & Burch, S. N. (2020). Acid sulfate soils: Formation. In B. D. Fath & S. E. Jorgensen (Eds.), *Managing Soils and Terrestrial Systems*. CRC Press.
- Rasoulina, P., & Mousavi, M. (2016). V and Ni recovery from a vanadium-rich power plant residual ash using acid producing fungi: *Aspergillus niger* and *Penicillium simplicissimum*. *RSC Advances*, *6*(11), 9139–9151. <https://doi.org/10.1039/C5RA24870A>
- Reich, M., Kesler, S. E., Utsunomiya, S., Palenik, C. S., Chryssoulis, S. L., & Ewing, R. C. (2005). Solubility of gold in arsenian pyrite. *Geochimica et Cosmochimica Acta*, *69*(11), 2781–2796. <https://doi.org/10.1016/j.gca.2005.01.011>
- Remy, W., Taylor, T. N., Hass, H., & Kerp, H. (1994). 4-hundred-million-year-old vesicular-arbuscular mycorrhizae. *Proceedings of the National Academy of Sciences, USA*, *91*(25), 11841–11843. <https://doi.org/10.1073/pnas.91.25.11841>
- Riaz, M., Kamran, M., Fang, Y., Wang, Q., Cao, H., Yang, G., et al. (2021). Arbuscular mycorrhizal fungi-induced mitigation of heavy metal phytotoxicity in metal contaminated soils: A critical review. *Journal of Hazardous Materials*, *402*, 123919. <https://doi.org/10.1016/j.jhazmat.2020.123919>
- Rice, C. M., Ashcroft, W. A., Batten, D. J., Boyce, A. J., Caulfield, J. B. D., Fallick, A. E., et al. (1995). A Devonian auriferous hot spring system, Rhynie, Scotland. *Journal of the Geological Society*, *152*(2), 229–250. <https://doi.org/10.1144/gsjgs.152.2.0229>
- Rice, C. M., & Trewin, N. H. (1988). A Lower Devonian gold-bearing hot-spring system, Rhynie, Scotland. *Transactions of the Institution of Mining and Metallurgy*, *97*, B141–B144.
- Rice, C. M., Trewin, N. H., & Anderson, L. I. (2002). Geological setting of the Early Devonian Rhynie cherts, Aberdeenshire, Scotland: An early terrestrial hot spring system. *Journal of the Geological Society*, *159*(2), 203–214. <https://doi.org/10.1144/0016-764900-181>
- Santelli, C. M., Webb, S. M., Dohnalkova, A. C., & Hansel, C. M. (2011). Diversity of Mn oxides produced by Mn(II)-oxidizing fungi. *Geochimica et Cosmochimica Acta*, *75*(10), 2762–2776. <https://doi.org/10.1016/j.gca.2011.02.022>
- Šebesta, M., Nemček, L., Urík, M., Kolenčík, M., Bujdoš, M., Hagarová, I., & Matúš, P. (2020). Distribution of TiO₂ nanoparticles in acidic and alkaline soil and their accumulation by *Aspergillus niger*. *Agronomy*, *10*(11), 1833. <https://doi.org/10.3390/agronomy10111833>
- Shangguan, Y., Qin, X., Zhao, L., Wang, L., & Hou, H. (2016). Effects of iron oxide on antimony(V) adsorption in natural soils: Transmission electron microscopy and X-ray photoelectron spectroscopy measurements. *Journal of Soils and Sediments*, *16*(2), 509–517. <https://doi.org/10.1007/s11368-015-1229-9>
- Shaw, R. A., & Goodenough, K. M. (2013). *The potential for indigenous niobium-tantalum resources in the Highlands of Scotland: A reconnaissance study. Internal Report IR/13/054*. British Geological Survey.
- Sheldrake, M. (2019). *Entangled Life*. Random House.
- Simmons, S. F., Kirby, S. H., Verplanck, P. L., & Kelley, K. D. (2018). Strategic and critical metals in produced geothermal fluids from Nevada and Utah. In *Paper presented at 43rd Workshop on Geothermal Reservoir Engineering, Stanford, California, February 12–14, 2018* (pp. 1–12).
- Smith, C. G., Livingstone, A., & Highton, A. J. (2019). Chapter 4. Scottish mineral Geological Conservation Review sites—Magmatic and skarn minerals. *Proceedings of the Geologist's Association*, *133*(4–5), 1–17. <https://doi.org/10.1016/j.pgeola.2019.10.006>
- Stefánsson, A., & Arnórsson, S. (2005). The geochemistry of As, Mo, Sb, and W in natural geothermal waters, Iceland. In *Proceedings of the World Geothermal Congress, Antalya, Turkey, 24–29 April 2005* (pp. 1–7).
- Strullu-Derrien, C., Goral, T., Longcore, J. E., Olesen, J., Kenrick, P., & Edgecombe, G. D. (2016). A new Chytridiomycete fungus intermixed with Crustacean Resting Eggs in a 407-million-year-old continental freshwater environment. *PLoS One*, *11*(12), e0167301. <https://doi.org/10.1371/journal.pone.0167301>
- Strullu-Derrien, C., Kenrick, P., Pressel, S., Duckett, J. G., Rioult, J.-P., & Strullu, D.-G. (2014). Fungal associations in *Horneophyton ligneri* from the Rhynie Chert (c. 407 million year old) closely resemble those in extant lower land plants: Novel insights into ancestral plant–fungus symbioses. *New Phytologist*, *203*(3), 964–979. <https://doi.org/10.1111/nph.12805>
- Suda, A., & Makino, T. (2016). Functional effects of manganese and iron oxides on the dynamics of trace elements in soils with a special focus on arsenic and cadmium: A review. *Geoderma*, *270*, 68–75. <https://doi.org/10.1016/j.geoderma.2015.12.017>
- Sudová, R., Jurkiewicz, A., Turnau, K., & Vosátka, M. (2007). Persistence of heavy metal tolerance of the arbuscular mycorrhizal fungus *Glomus intraradices* under different cultivation regimes. *Symbiosis*, *43*, 71–81.
- Syrvatka, V., Rabets, A., Gromyko, O., Luzhetskyy, A., & Fedorenko, V. (2022). Scandium–microorganism interactions in new biotechnologies. *Trends in Biotechnology*, *40*(9), 1088–1101. <https://doi.org/10.1016/j.tibtech.2022.02.006>
- Taylor, T. N., Klavins, S. D., Krings, M., Taylor, E. L., Kerp, H., & Hass, H. (2004). Fungi from the Rhynie Chert: A view from the dark side. *Transactions of the Royal Society of Edinburgh Earth Sciences*, *94*(4), 457–473. <https://doi.org/10.1017/s026359330000081x>
- Thompson, I. A., Huber, D. M., Guest, C. A., & Schulze, D. G. (2005). Fungal manganese oxidation in a reduced soil. *Environmental Microbiology*, *7*(9), 1480–1487. <https://doi.org/10.1111/j.1462-2920.2005.00842.x>
- Trewin, N. H. (1994). Depositional environment and preservation of biota in the Lower Devonian hot-springs of Rhynie, Aberdeenshire, Scotland. *Transactions of the Royal Society of Edinburgh Earth Sciences*, *84*(3–4), 433–442. <https://doi.org/10.1017/s0263593300006234>
- Trewin, N. H., & Fayers, S. R. (2015). Macro to micro aspects of the plant preservation in the Early Devonian Rhynie cherts, Aberdeenshire, Scotland. *Earth and Environmental Science Transactions of the Royal Society of Edinburgh*, *106*(2), 67–80. <https://doi.org/10.1017/s1755691016000025>
- Tullio, M., Pierandrei, F., Salerno, A., & Rea, E. (2003). Tolerance to cadmium of vesicular arbuscular mycorrhizae spores isolated from a cadmium polluted and unpolluted soil. *Biology and Fertility of Soils*, *37*(4), 211–214. <https://doi.org/10.1007/s00374-003-0580-y>
- Ullrich, M. K., Pope, J. G., Seward, T. M., Wilson, N., & Planer-Friedrich, B. (2013). Sulfur redox chemistry governs diurnal antimony and arsenic cycles at Champagne Pool, Waitapu, New Zealand. *Journal of Volcanology and Geothermal Research*, *262*, 164–177. <https://doi.org/10.1016/j.jvolgeores.2013.07.007>
- Wacey, D., Kilburn, M. R., Saunders, M., Cliff, J. B., Kong, C., Liu, A. G., et al. (2015). Uncovering framboidal pyrite biogenicity using nano-scale CN_{org} mapping. *Geology*, *43*(1), 27–30. <https://doi.org/10.1130/g36048.1>
- Wei, Y., Su, Q., Sun, Z., Shen, Y., Li, J., Zhu, X., et al. (2016). The role of arbuscular mycorrhizal fungi in plant uptake, fractions, and speciation of antimony. *Applied Soil Ecology*, *107*, 244–250. <https://doi.org/10.1016/j.apsoil.2016.04.021>

- Wellman, C. H. (2006). Spore assemblages from the Lower Devonian 'Lower Old Red Sandstone' deposits of the Rhynie outlier, Scotland. *Transactions of the Royal Society of Edinburgh Earth Sciences*, 97(2), 167–211. <https://doi.org/10.1017/s0263593300001449>
- Zhang, X., Ren, B. H., Wu, S. L., Sun, Y. Q., Lin, G., & Chen, B. D. (2015). Arbuscular mycorrhizal symbiosis influences arsenic accumulation and speciation in *Medicago truncatula* L. in arsenic-contaminated soil. *Chemosphere*, 119, 224–230. <https://doi.org/10.1016/j.chemosphere.2014.06.042>
- Zhao, F. J., Ma, J. T., Meharg, A. A., & McGrath, S. P. (2009). Arsenic uptake and metabolism in plants. *New Phytologist*, 181(4), 777–794. <https://doi.org/10.1111/j.1469-8137.2008.02716.x>